Bioorthogonal antigens as tool for investigation of antigen processing and presentation

Pieper Pournara, L.

Citation

Pieper Pournara, L. (2021, November 16). *Bioorthogonal antigens as tool for investigation of antigen processing and presentation*. Retrieved from https://hdl.handle.net/1887/3239301

Version:	Publisher's Version
License:	Licence agreement concerning inclusion of doctoral thesis in the Institutional Repository of the University of Leiden
Downloaded from:	https://hdl.handle.net/1887/3239301

Note: To cite this publication please use the final published version (if applicable).
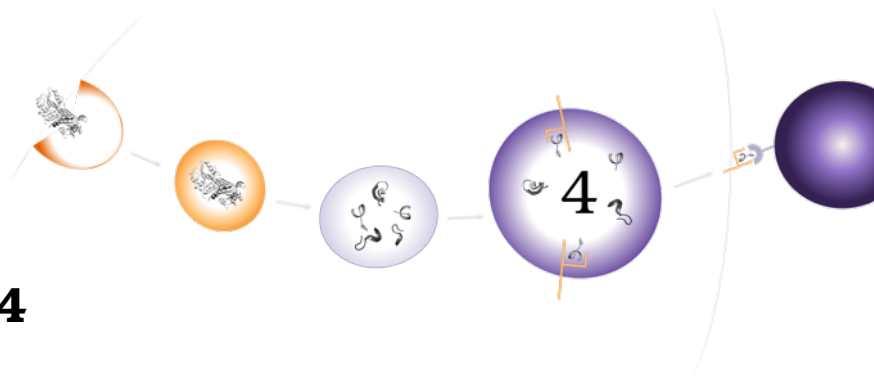
Chapter 4

In vitro protein degradation of bioorthogonal antigens

4.1 Introduction

MHC-II restricted peptides are generated through the concerted action of endo-lysosomal proteases. These proteases are structurally heterogeneous, but have certain residues in their active site. The main families of relevance for this chapter are the cysteine, serine and aspartyl proteases, many of which have a papain-like fold and are of the cathepsin family[89,108]. The biology of these proteases is quite complex: each protease has its own specific activity maximum at a certain pH range (see Table 4.1) and the expression levels between the proteases varies between immune cells, and over time[95,249,250], as has been determined by activity based protein profiling, Western blotting and fluorogenic substrate assays[251-253]. Their production as zymogens - that are only activated in the endo-lysosomal system by the local acidic environment and/or the action of proteases already present further complicates matters.

Table 4.1: Protease selectivity based on individual amino acids. Amino acid preference for highest overall cleavage specificity per position counting 4 amino acids upstream (P) and 4 amino acids downstream (P') of the respective endo-lysosomal protease cleavage site (the scissile bond) and optimal pH range.

Protease	P4	P3	P2	P1	P1'	P2'	P3'	P4'	pH range
Asparagine endopeptidase	-	-	-	**asn**, asp	-	-	-	-	4.0-6.0
Cathepsin D	-	-	-	**leu**, phe	-	-	-	-	2.8-4.0
Cathepsin L	-	-	leu, val, ile	-	-	-	-	-	6.0
Cathepsin S	-	-	leu, val	-	-	-	-	-	6.0

Bold amino acid shows a higher preference compared to non-bold amino acid. Source: Rawlings *et al.* (2014/2018)[254,255] and the MEROPS library of peptidases. asn=asparagine, asp=aspartic acid, leu=leucine, phe=phenylalanine, val=valine, ile=isoleucine

As described in Chapter 2.1.1, the role of specific proteases in antigen presentation has been extensively studied. These studies have culminated in detailed understanding
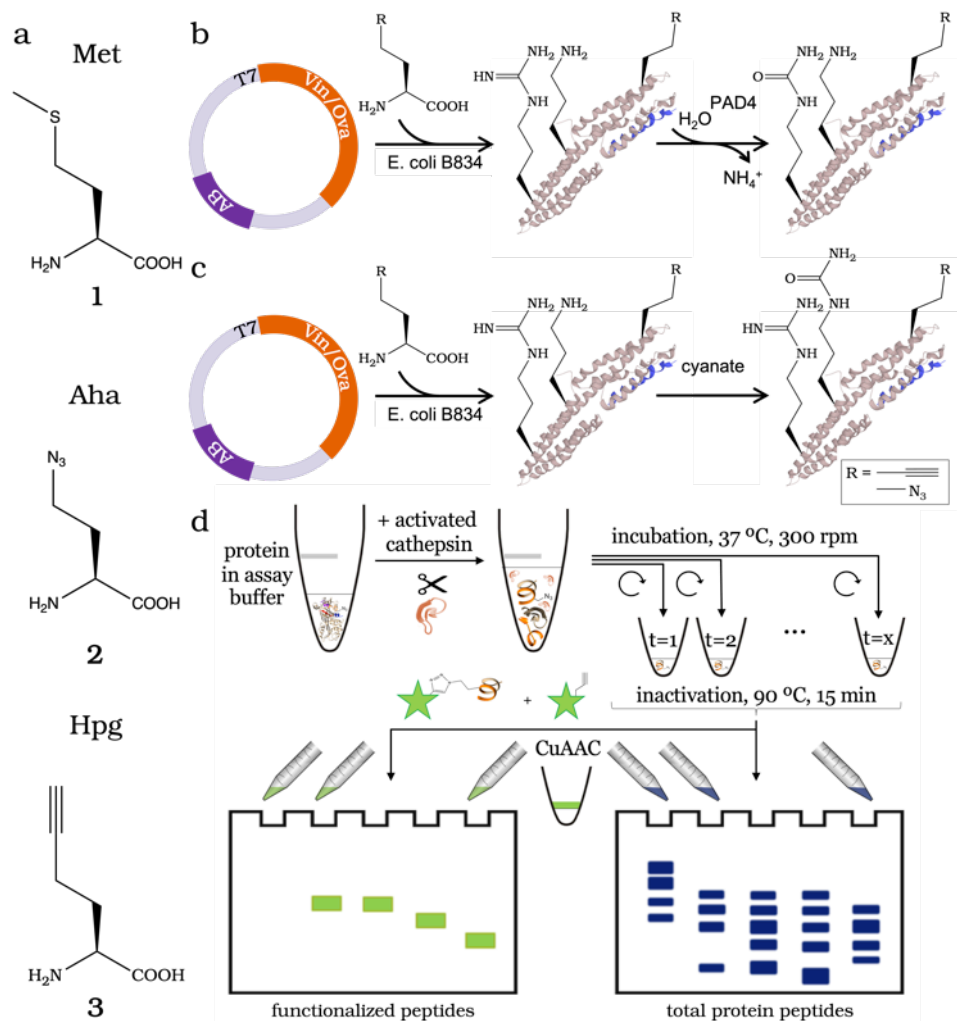
Figure 4.1: Scheme for recombinant truncated human vinculin$_{435-743}$ production, their post-translational modification and assay workflow. (a) Chemical structures for (**1**) methionine (Met), (**2**) azidohomoalanine, (**3**) homopropargylglycine, (b) citrullination of Vin, (c) carbamylation of Vin, (d) scheme of the workflow of *in vitro* degradation of protein antigens. Recombinant proteases are activated in respective activation buffer for a specific time depending on the protease and mixed with protein in assay buffer, also depending on the protease used. The samples are then incubated at optimal temperature on a shaker. Equal amounts of protein are removed from the reaction at indicated time intervals and proteases are inactivated by heat. Samples were split for analysis of the samples by SDS-PAGE measuring total protein content and fragmentation pattern by e.g., Coomassie staining or silver staining (whole protein), and for the bioorthogonal antigens after performing a click reaction (CuAAC) with the respective functionalized fluorophore (functionalized protein). T7 = promotor, Vin = vinculin, Ova = ovalbumin, AB = antibiotic, PAD4 = protein arginine deiminase 4, NH_4^+ = ammonium cation.

of certain aspects of this pathway, such as the role of individual proteases in the cleavage of CD74 that leads to the maturation of the MHC-II complex to a peptide receptive state.

One thing that cannot yet be reliably predicted, however, is the role of specific proteases in liberating the MHC-II restricted epitope peptides from antigenic proteins: why some peptides emerge from this overall process to be loaded on MHC-II, and others that would bind equally well are proteolytically destroyed remains unknown. This lack of knowledge is in part due to the broad substrate specificity of most of the endo-lysosomal proteases. Also, changes in cleavage rates within different endosomal compartments (mostly influenced by pH), and the folding state of the antigen all affect the rate of proteolysis and antigen liberation.

Changes in the rate of proteolysis and the nature of the cleavage site have been implicated in the pathogenesis of certain auto-immune diseases. It has, for example, been shown that the elimination of one specific protease (asparagine endopeptidase, AEP) can lead to the disappearance of certain epitopes from TTcF[90]. This was also shown for cathepsin B (CatB)[256], cathepsin L (CatL)[257], and cathepsin S (CatS)[258] in the degradation and peptide liberation from the model antigen, hen egg lysozyme (HEL)[259], immune complexes[260]. Elimination of either of the three cathepsins can indeed lead to altering the complete repertoire of MHC II-presented peptides in model systems[261].

The inhibition or elimination of proteases does not just reduce the presentation of antigenic peptides, but can also lead to the appearance of new epitopes. A key T cell auto-antigenic peptide of the multiple sclerosis auto-antigen MBP is destroyed under normal processing conditions, but is presented efficiently in AEP$^{-/-}$ APCs[262] - APCs derived from mice genetically deficient for both AEP alleles. Similarly, destructive roles have been attributed to cathepsin D (CatD)[116], with its inhibition leading to an increased presentation of a myoglobin T cell epitope.

Intriguingly, it has been posed that PTM, such as citrullination, that occur during auto-immune pathogenesis of multiple sclerosis can lead to the appearance (and/or disappearance) of T cell epitopes that drive the B cell maturation seen in this disease affecting the central nervous system (CNS)[111]. In this case cathepsin H[263,264] was implicated, although the involvement of other proteases could not be excluded.

One conclusion that can be drawn from the above examples is that no general trends linking proteolytic stability and the appearance of new T cell epitopes can be drawn and in order to determine whether a specific modification of a protein alters its processing rate, a detailed in vitro characterization must be performed. This was the aim of the research described in this chapter: to get insights into whether the PTM of lysine to homocitrulline, or that of arginine to citrulline, of the auto-antigen vinculin (Vin) alters its proteolytic susceptibility.

Vin is a 117 kDa cytoskeletal adapter protein that is found in the synovial fluid of patients suffering from rheumatoid arthritis[265]. Most interestingly, the antibody responses against this protein found in these patients are directed against citrullinated and/or carbamylated variants of this antigen[266]. The heavy chains of these antibodies are non-IgM/IgD, indicating the involvement of a T cell response in the maturation of the B cells that produce these antibodies[267,268]. Despite such a T cell having not yet been found, it is hypothesized that the PTMs of Vin could lead to the appearance of a neo-epitope due to altered proteolysis resulting from these PTMs. The aim was therefore to assess whether PTMs of Vin can alter the susceptibility of the antigen to some of the above-mentioned proteases. This opens also the way to assess, if this has impact also on T cell epitope production (Figure 4.1[214]). An additional aim of this chapter

is to determine whether the introduction of bioorthogonal Met-analogues into proteins (Chapter 3) alters the proteolytic susceptibility of an antigen to a given protease, which would limit their use as model reagents for the study of degradation in cells.

4.2   Results

In order to address the above-described aims, recombinant variants of vinculin were expressed; either as the wildtype protein, or carrying the bioorthogonal Met-analogues Aha or Hpg at the 8 Met-Codon sites in the protein (produced as described in Chapter 3), before post-translationally converting their Arg→Cit residues or their Lys→Carb residues. This matrix of 9 proteins (Table 4.2, Figure 4.1) was then incubated with a series of recombinant endo-lysosomal proteases (with either AEP, CatD, CatL or CatS) and the rate of degradation determined for each of these.

Table 4.2: Recombinant protein variants and modifications. Details of all recombinant protein variants produced. Vinculin without modification, carbamylated vinculin and citrullinated Vinculin, molecular weight and the percentage of unnatural amino acid incorporation or modification respectively.

| Protein	Name	Molecular weight (Da)	% labelling / modification
1	Met-Vin	35 890.0	n.a.
2	Aha-Vin	35 714.6	90-100% [*]
3	Hpg-Vin	35 578.6	90-100% [*]
4	carb_Met-Vin	§	74-100%
5	carb_Aha-Vin	§	74-100%
6	carb_Hpg-Vin	§	74-100%
7	cit_Met-Vin	*	[+]
8	cit_Aha-Vin	35 736.0	[+]
9	cit_Hpg-Vin	35 668.0	[+]

[*]in some cases the start-Met is cleaved off after expression. §mixed species from 17 to 23 carbamylation sites per protein molecule. *no reliable mass data could be obtained for this protein to date. [+]can not be determined because the mass difference of only 1 Da is too small to prove success of modification. Presence of citrullination was proven by ACPA-ELISA[214,223].

The conditions for degradation were standardized as much as possible across all experiments as follows: The Vin-variants were used at 10 μM and incubated with each protease in the assay buffer as suggested by the supplier at 37 °C (see Table 4.4 in Section 4.4.2 for details). For analysis samples were taken at the indicated times after start of digest and separated on SDS-PAGE. The gels were silver-stained to allow the visualization of fainter bands.

A recombinant truncated version of Vin comprising amino acid residues 435-743 was expressed in the methionine auxotrophic strain *E. coli* B834 as previously described[269]. Medium was supplemented either with Met (**1**) or replaced by the UAAs Aha (**2**) or Hpg (**3**) prior to induction of expression with IPTG. The resulting recombinant Vin

proteins, which had a molecular weight of 36 kDa, contained 8 Met-codons (excluding the start codon) of which 7-8 were replaced by Aha-Vin or Hpg-Vin as determined by MS (the remaining codon still containing a Met-residue). Next, the structures of the bioorthogonal variants were compared to that of the wildtype (Met-Vin) by CD. Minimal structural differences were observed between the three, although an increase in ellipticity (∂) was observed for the Hpg-analogue, suggesting a stabilization of the protein fold (Figure 4.2[223]).
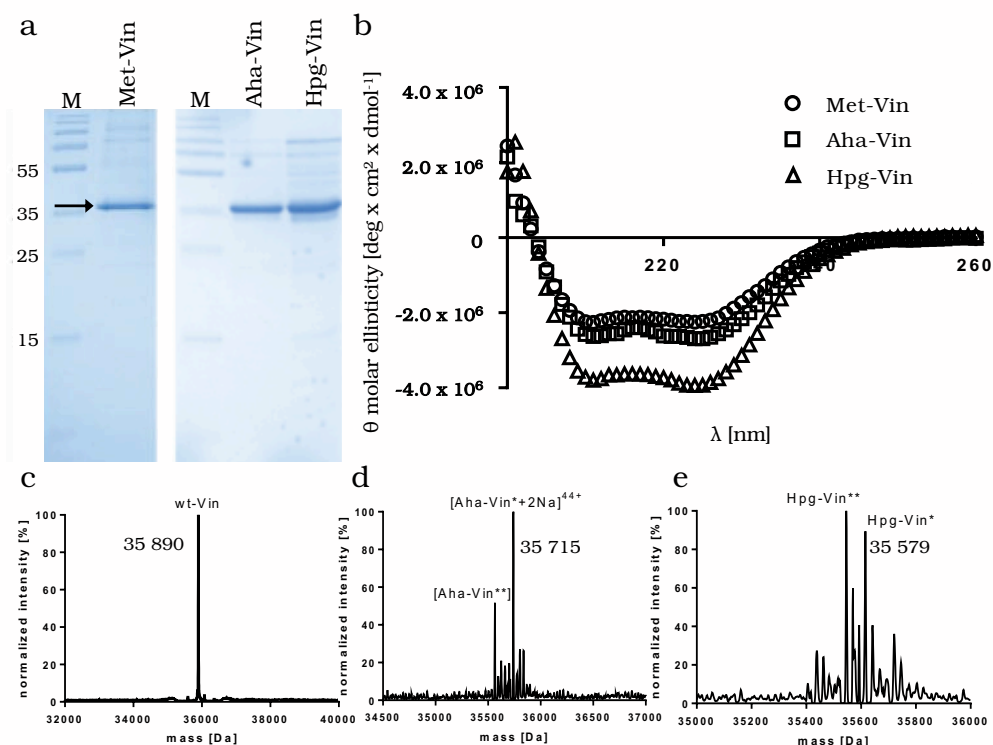

Figure 4.2: Characterization of recombinant truncated human vinculin$_{435-743}$. (a) SDS-PAGE analysis of purified, non-modified recombinant Vin (Met-Vin) and the bioorthogonal derivatives (Aha-Vin and Hpg-Vin) at 36 kDa ($\rightarrow$). (b) Circular dichroism of purified bioorthogonal antigens for analysis of correct secondary structure of the protein after production and purification. Met-Vin (circles), Aha-Vin (squares) and Hpg-Vin (triangles). ToF-MS analysis of (c) non-modified recombinant Vin (Met-Vin, expected mass: 35 886 Da, observed mass: 35 890 Da) (d) recombinant bioorthogonal Aha-Vin (Aha-Vin, expected mass: 35 715 Da, observed mass: 35 714.6 Da (Aha-Vin **) and 35 759 Da (Aha-Vin *+2Na^{44+})) (e) recombinant bioorthogonal Hpg-Vin (Hpg-Vin, expected mass: 35 579 Da, observed mass: 35 578.6 Da (Hpg-Vin **) and 35 759 Da (Hpg-Vin *+2Na^{44+}))

4.2.1 Post-translational modification of vinculin

To allow the study of whether post-translational citrullination and carbamylation would alter processing of this antigen, citrullinated and carbamylated forms were generated *in vitro* for all three variants of Vin using previously described procedures (Figure 4.1 and Table 4.2).

4.2.2 Analysis of the degradation of bioorthogonal variants

After the three different protein variants were prepared they were used for the *in vitro* degradation experiments with different proteases as shown in the work flow scheme in Figure 4.1d.

(a) asparagine endopeptidase   **(b)** cathepsin D
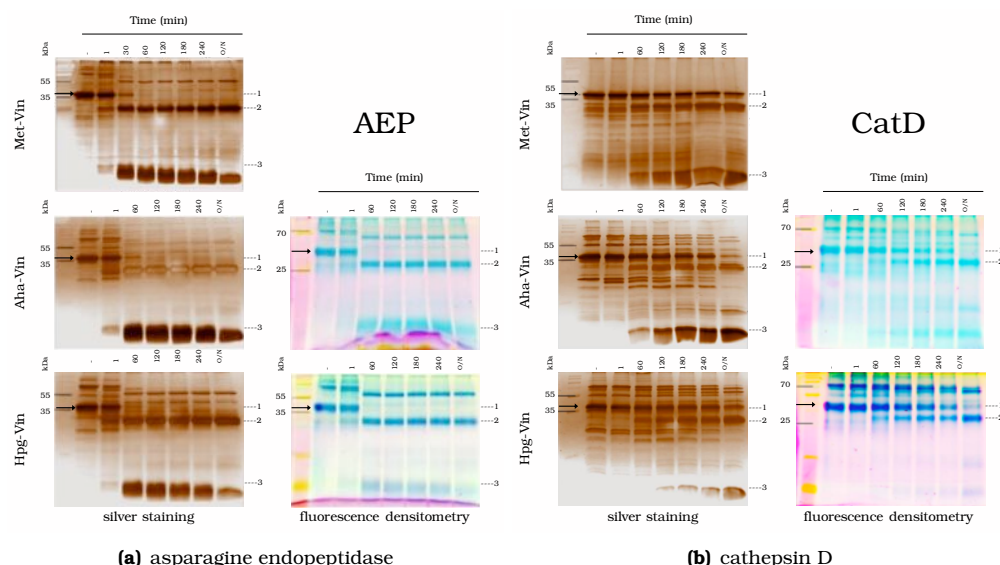
Figure 4.3: Silver staining and fluorescence densitometry of the digest of vinculin with asparagine endopeptidase and cathepsin D. (a) 10 μM of protein were digested over time (min) with 40.8 nM (>0.5 U/ml) AEP in 50 mM MES, 250 mM NaCl, pH 5.0. Silver staining: Met-Vin, Aha-Vin and Hpg-Vin were digested with samples being taken at the indicated times and run on SDS-PAGE. Fluorescence densitometry: Aha-Vin and Hpg-Vin were digested. Taken samples were ligated with (d) Cy5-alkyne and (e) TAMRA-azide and run on SDS-PAGE. (b) 10 μM of protein were digested over time (min) with 18.18 nM (>0.48 U/ml) CatD in 100 mM NaOAc, 200 mM NaCl, pH 3.5. Silver staining: Met-Vin, Aha-Vin and Hpg-Vin were digested with samples being taken at the indicated times and run on SDS-PAGE. Fluorescence densitometry: Aha-Vin and Hpg-Vin were digested. Taken samples were ligated with Cy5-alkyne and TAMRA-azide and run on SDS-PAGE. (-) negative control without protease, ($\rightarrow$, -1) intact protein, (-2)-(-3) main digestion fragments, (O/N) over night, (kDa) molecular weight standard.

The respective amount of each protein was dissolved in assay buffer to a concentration of 20 μM, the respective amount of active protease units was added in equal volume of assay buffer to yield the final concentration of protein. Digestion was performed at 37 °C on a shaker and samples for digest were taken at the indicated time points. Active protease was heat-inactivated at 90 °C and ccHc-reaction was performed with

(a) cathepsin L
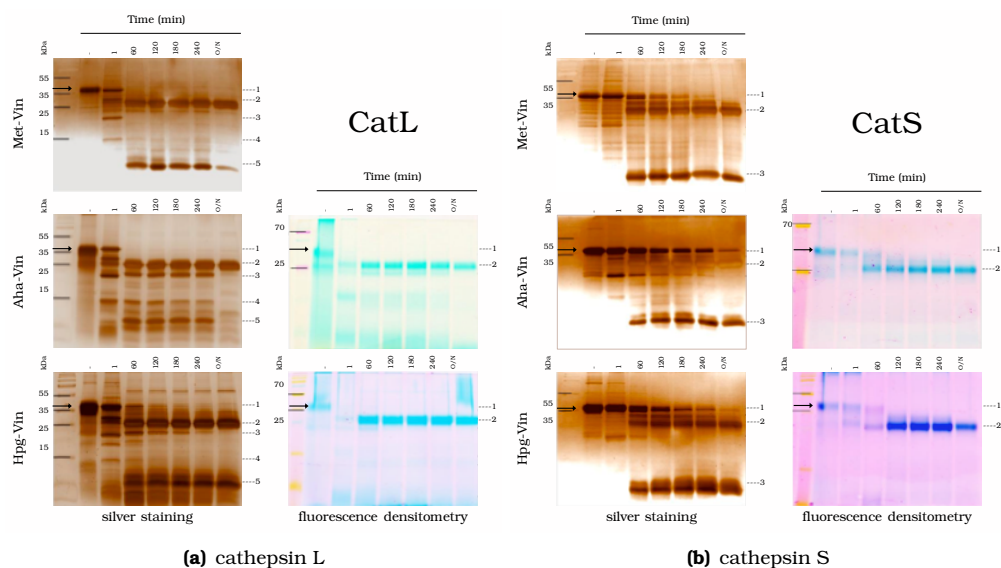
(b) cathepsin S

Figure 4.4: Silver staining and fluorescence densitometry of the digest of vinculin with cathepsin L and cathepsin S. (a) 10 μM of protein were digested over time (min) with 2.7 nM (>0.5 U/ml) CatL in 25 mM MES, 5 nM DTT, pH 6.0. Silver staining: Met-Vin, Aha-Vin and Hpg-Vin were digested with samples being taken at the indicated times and run on SDS-PAGE. Fluorescence densitometry: Aha-Vin and Hpg-Vin were digested. Taken samples were ligated with Cy5-alkyne and TAMRA-azide and run on SDS-PAGE. (b) 10 μM of protein were digested over time (min) with 25.64-35.72 nM (>0.3 U/ml) CatS in 50 mM NaOAc, 5 mM DTT, 250 mM NaCl, pH 4.5. Silver staining: Met-Vin, Aha-Vin and Hpg-Vin were digested with samples being taken at the indicated times and run on SDS-PAGE. Fluorescence densitometry: Aha-Vin and Hpg-Vin were digested. Taken samples were ligated with Cy5-alkyne and TAMRA-azide and run on SDS-PAGE. (-) negative control without protease, ($\rightarrow$, -1) intact protein, (-2)-(-4) main digestion fragments, (O/N) over night, (kDa) molecular weight standard.

the respective fluorophore. Then samples were prepared for SDS-PAGE analysis. Subsequently, fluorescent densitometry showed the fluorescently labelled protein bands, after which a standard silver staining was performed to show all protein bands.

The digest of Vin by AEP, showed similar rates of degradation for the wildtype (Met-Vin) and bioorthogonal variants (Aha-Vin and Hpg-Vin) of the protein (Figure 4.3a). The intact protein band was lost between 60-120 min with the appearance of two main fragments at ~27 kDa (-2) and at ~10 kDa (-3) occurring rapidly (at the t = 1 min time point). Fragment 2 was still not digested further after over night incubation, while fragment 3 appeared to get further degraded by one or a few amino acids at a time causing a gradual lowering of the band with decreasing molecular weight over time.

A fraction of each sample was also treated with the appropriate bioorthogonal fluorophore (Cy5-alkyne for Aha-Vin and and TAMRA-azide for Hpg-Vin) to effect labelling of these bioorthogonal amino acids with a fluorophore (Figure 4.3a, right panel). Fluorescence was measured in the gel at the respective wavelength. The fluorescence densitometry measurements showed similar degradation patterns compared to the silver staining, however, often times not all fragments. Strong difference in fluorescence

(a) Met-Vin comparison   **(b)** citrullination   **(c)** carbamylation
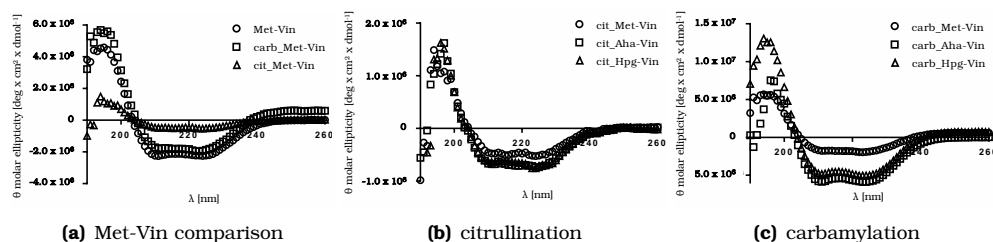
Figure 4.5: Biophysical characterization of non-modified, carbamylated and citrullinated Met-Vin, Aha-Vin and Hpg-Vin by circular dichroism spectroscopy. Circular dichroism of purified bioorthogonal antigens for analysis of correct secondary structure of the protein after production and purification. (a) Comparison of Met-Vin with cit_Met-Vin and carb_Met-Vin; Met-Vin (circles), cit_Met-Vin (squares) and carb_Met-Vin (triangles). (b) Comparison of cit_Met-Vin with citrullinated bioorthogonal Vin variants; Met-Vin (circles), cit_Aha-Vin (squares) and cit_Hpg-Vin (triangles). (c) Comparison of carb_Met-Vin with both bioorthogonal Vin variants; carb_Met-Vin (circles), carb_Aha-Vin (squares) and carb_Hpg-Vin (triangles).

intensity could indicate, which fragments contained more or less bioorthogonal amino acids with attached fluorophores, respectively. According to this rationale, (more) UAAs were present in the ~27 kDa fragment (-2) compared to the smaller ~10 kDa fragment (-3). Additional bands visible above the intact protein with size of ~75 kDa and ~60 kDa, are likely due to impurities or aggregates of the protein.

Incubation of Vin with CatD under conditions as described above for AEP (Figure 4.3b) revealed the very slow degradation of all three variants with this protease. The first fragments appeared at 60 min with a molecular weight of ~27 kDa (-2) and ~10 kDa (-3), but the undigested protein band remained visible until the over night time point. One breakdown product was observed when Aha-Vin and Hpg-Vin were treated with CatD, with the formation of a single fragment ~27 kDa (-2) for both bioorthogonal constructs.

A fraction of each sample was again used to perform the CuAAC-reaction. SDS PAGE separation of these samples was now followed by fluorescence densitometry to determine whether or not breakdown products contain bioorthogonal amino acids, or in other words, contain sites where in the wildtype protein methionines would be present (Figure 4.3b, right panel). Similar as for the digest with AEP, the digest with CatD showed comparable degradation patterns for both measurements, except for the smaller ~10 kDa fragment (-3).

CatL did affect the rapid disappearance of the 36 kDa Vin band ($\rightarrow$, < 1 h; Figure 4.4a) with the appearance of two persisting main bands at ~25-30 kDa (-2, -3) and one persisting main band at a low molecular weight ~10 kDa (-4). In between a plethora of minor degradation fragment bands of varying size and with varying persistence appeared for all three Vin variants. CatL completely degraded all Vin protein variants (-1) between 1-60 min, similar as for AEP. The fluorescence densitometry measurement showed only the fragment ~30 kDa (-2, Figure 4.4a, right panel).

For digest with CatS all three forms showed the formation of two persisting bands, one at ~30 kDa (-2) and a smaller fragment at ~10 kDa (-3), that persisted for the remainder of the experiment (Figure 4.4b). As for CatD, the digest of Vin with CatS was slower compared to AEP and CatL. The fluorescence densitometry measurement

showed only the fragment at ~30 kDa (-2) for Aha-Vin and Hpg-Vin, while the other fragments were not visible (Figure 4.4b, right panel).

4.2.3   Digest of post-translationally modified vinculin variants

Having shown that the bioorthogonal variants showed similar degradation patterns compared to Met-Vin, it was next assessed whether citrullination of Arg and the carbamylation of Lys affected the stability towards the above proteases. First CD was used to assess the secondary structure (Figure 4.5). Carbamylation led to stabilization of the tertiary structure as indicated by CD, whereas citrullination yielded variants that were rich in β-sheet content and random coil-rich with a simultaneous decrease of a-helical character[223].

4.2.4   Digest of carbamylated vinculin variants

Carbamylation strongly affected the degradation by AEP. carb_Met-Vin, carb_Aha-Vin and carb_Hpg-Vin were not degraded at all, even after over night incubation (Figure 4.6, carb_Met-Vin not shown).

In vitro degradation assays, as analysed by silver staining and CuAAC followed by in-gel fluorescence densitometry (as described before), showed that carbamylation causes a slowdown of the degradation by AEP, and to a lesser extent CatL and CatS. Susceptibility to CatD degradation, on the other hand quickened, with the intact protein band having disappeared after over night incubation (Figure 4.6).

4.2.5   Digest of citrullinated bioorthogonal vinculin variants

Citrullination of Vin had less of an effect on the rate of degradation. No differences were observed for the degradation by AEP and CatL upon citrullination (Figure 4.7), neither by silver stain analysis nor by fluorescence analysis. Incubation with CatD, did cause a change in proteolytic susceptibility. Where Met-Vin was fully stable to CatD degradation (see Figure 4.3b), cit_Met-Vin (and its bioorthogonal variants) were degraded upon incubation with CatD.
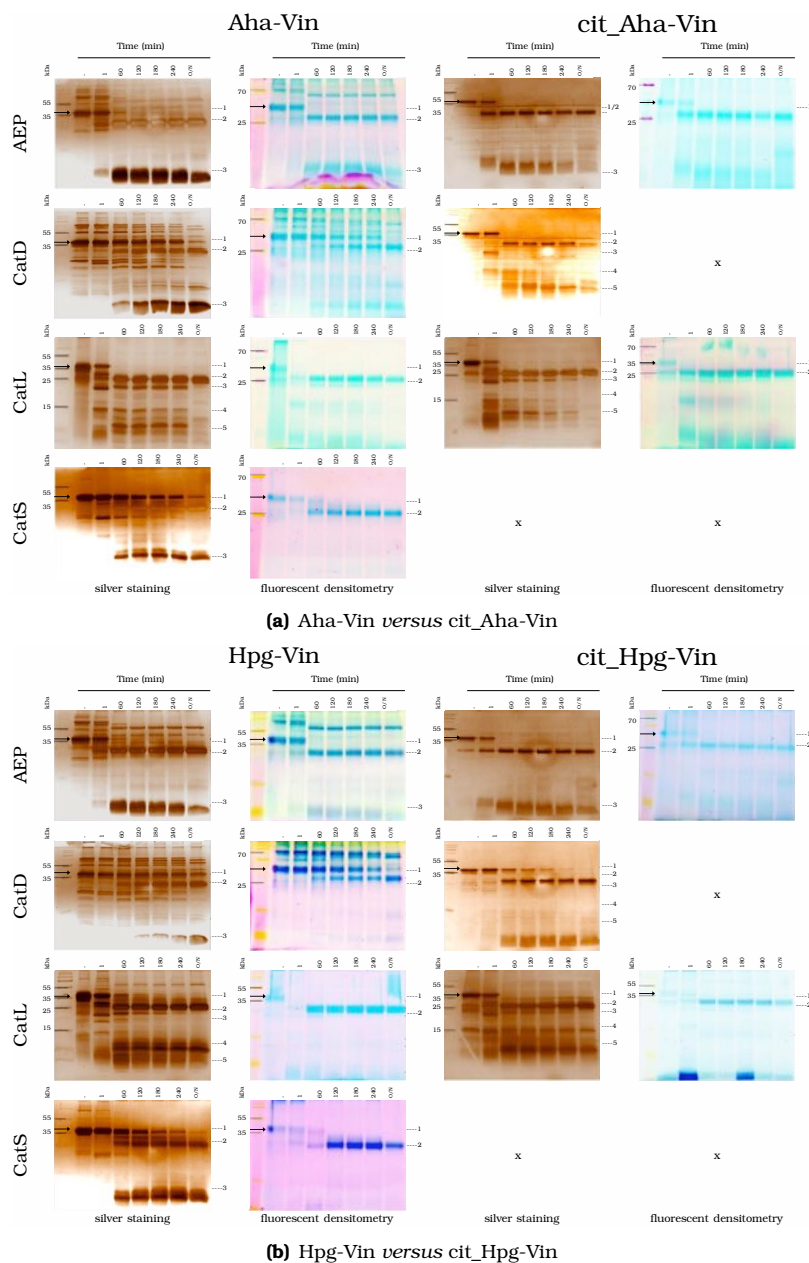
These experiments show that the influence of citrullination on the protein degradation in comparison to the non-modified protein is highly protease dependent: carbamylation slowed down the degradation by AEP, and to a lesser extent CatL, whereas citrullination increased susceptibility to proteolytic degradation by CatD, but not for AEP and CatL.

4.2.6   Digest of fluorescently labelled bioorthogonal vinculin variants

Having confirmed that the bioorthogonal proteins were similarly degraded to wildtype counterparts, it was next assessed whether introducing the fluorophores prior to the digestion with proteases altered their propensity to be degraded. To this end, the proteins were subject to CuAAC ligation with alkyne-Cy5 or azide-TAMRA fluorophore at 1 μM for 30 min, at rt in the dark, prior to purification by gel permeation chromatography to remove unreacted fluorophore and ligation reagents. These fluorophore-modified proteins were next subjected to proteolysis similar to the experiments described above and

(a) Aha-Vin *versus* carb_Aha-Vin

(b) Hpg-Vin *versus* carb_Hpg-Vin
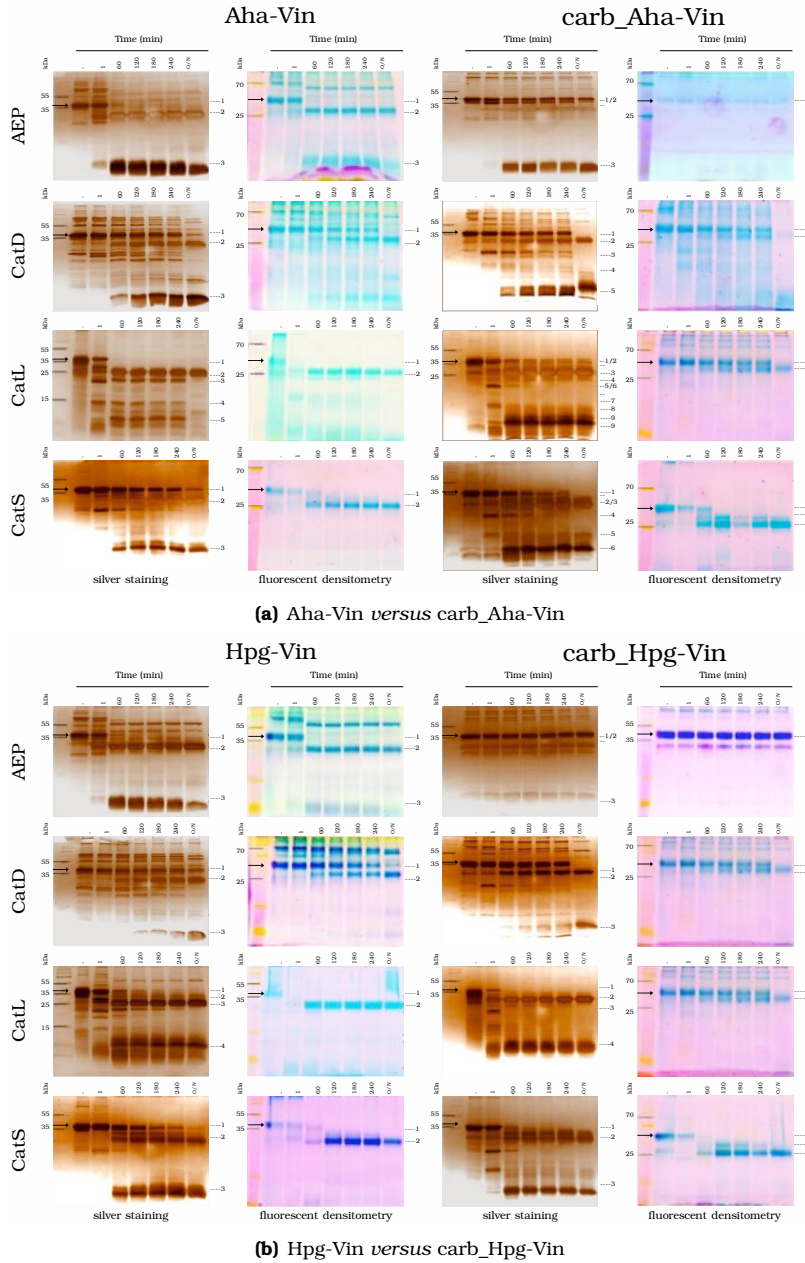
Figure 4.6: Silver staining and fluorescent densitometry of the digest of non-modified *versus* carbamylated vinculin with all used proteases. Bioorthogonal Vin and carb-Vin variants were digested over time (min) by AEP, CatD, CatL and CatS with samples being taken at the indicated times. Samples were run on SDS-PAGE with subsequent silver staining and fluorescent densitometry. (-) negative control without protease, (→, -1) intact protein, (-2)-(-10) main digestion fragments, (O/N) over night, (kDa) molecular weight standard.

(a) Aha-Vin *versus* cit_Aha-Vin

(b) Hpg-Vin *versus* cit_Hpg-Vin

Figure 4.7: Silver staining and fluorescent densitometry of the digest of non-modified *versus* citrullinated vinculin with all used proteases. Bioorthogonal Vin and cit-Vin variants were digested over time (min) by AEP, CatD, CatL and CatS with samples being taken at the indicated times. Samples were run on SDS-PAGE with subsequent silver staining and fluorescent densitometry. (-) negative control without protease, (→, -1) intact protein, (-2)-(-4) main digestion fragments, (O/N) over night, (kDa) molecular weight standard, x = result not available.

(a) Aha-Vin *versus* fluor_Aha-Vin

(b) Hpg-Vin *versus* fluor_Hpg-Vin

Figure 4.8: Silver staining and fluorescent densitometry of the digest of non-modified *versus* fluorescent vinculin with all used proteases. Biorthogonal Vin and *fluor_Vin* variants were digested over time (min) by AEP, CatD, CatL and CatS with samples being taken at the indicated times. Samples were run on SDS-PAGE with subsequent silver staining and fluorescence densitometry. (-) negative control without protease, (→, -1) intact protein, (-2)-(-4) main digestion fragments, (O/N) over night, (kDa) molecular weight standard.

analysed by silver staining and fluorescence densitometry. These experiments showed a complete abolition of degradation by AEP (Figure 4.8) and CatL. Degradation by CatS was less affected. Degradation with CatD was not performed due to time constraints.

4.3   Discussion and conclusion

In this chapter the influence of stability of protein substrates on proteolysis by different proteases was investigated. In order to do so the degradation speed and the fragmentation pattern of different proteins, and their modified counterparts, under different conditions were tested *in vitro* with selected recombinant proteases. It was hypothesized that more stable antigen proteins are more immunogenic, relating to or producing an immune response, and therefore cause enhanced T cell priming and/or antibody responses [84,119,270].

In summary, recombinant truncated Vin can be degraded by different recombinant lysosomal proteases. Bioorthogonal variants of Vin containing either Aha or Hpg bearing the respective bioorthogonal handle (azide or alkyne) were tested side by side with its non-bioorthogonal analogue. Additionally, all three variants were post-translationally modified on their lysine residues by either carbamylation, citrullination or by attaching a fluorophore. The degradation patterns observed were analysed in terms of persistence over time and digestion pattern. The introduction of the UAAs into the proteins caused minor differences in the degradation pattern and sometimes also in the persistence of certain breakdown fragments. These differences however were minor compared to the influence of PTMs on protease efficacy. PTM of the proteins did cause profound differences in both digestion speed and fragmentation for one protease, while it did not influence the digest by another (Table 4.3).

Table 4.3: Impact of post-translational modifications on *in vitro* degradation of biorthogonal antigens by recombinant proteases. Summary of the *in vitro* degradation of biorthogonal antigen variants by 4 recombinant endo-lysosomal proteases after carbamylation, citrullination or attachment of a fluorophore using click chemistry.

Protease	AEP	CatD	CatL	CatS
no modification	+++	+	+++	++
carbamylated	o	++	+/++	+/++
citrullinated	+++	+++	+++	-
fluorinated	o	-	++	++

rate of degradation: +++ = fast, ++ = moderate, + = slow,

o = no degradation, - = not determined.

The results show that the presence of protein modifications might have an influence on the protease activity, but that this influence is highly protease dependent. Through the PTM susceptibility of a certain substrate to degradation can be highly altered. The investigation of influence is very individual depending on each substrate and how many susceptible points exist within the amino acid chain.

For carbamylation, less degradation occurred for rhAEP, CatL and CatS while for CatD digest was accelerated slightly. To explain these differences, the nature of car-

bamylation on the physical properties of a protein has to be considered. As shown by CD the carbamylation caused a stabilization of the structure. Carbamylation, in contrast to citrullination, is the non-enzymatic post-translational modification (NEPTM). However, the results shown here indicate that carbamylation can influence protein degradation in the endo-lysosomal environment. For citrullination digestion went faster for CatD, while it did not change for rhAEP and CatL. Pre-labelling with a fluorophore showed resistance against degradation for rhAEP and partially for CatL, but not for CatS. The attachment of fluorophores to proteins or peptides caused unintended changes and effects. Modifications of the proteins showed prevention or promotion of degradation or even a change in the proteolytic site preference by the proteases. This makes the prediction of the influence of single or a combination of modifications very difficult.

Overall, the results show that the degradation speed was influenced only slightly by the incorporation of UAAs. Naturally occurring PTMs such as carbamylation and citrullination indeed can highly influence the degradation of proteins and that artificial reporter tags such as fluorophores have to be handled with care on a case-to-case bases. Dissenting with literature the conclusion is that increases proteolytical resistance does not correlate with increased stability of a protein[84,119], but that PTMs can prevent degradation due to physically blocking of access to cleavage sites[90] was confirmed. However, all tested factors, proteolytic stability and proteolytic preferences, differ between proteases. The synergy of the spheric influence of each proteases makes the endo-lysosomal pathway so effective and important but at the same time so difficult to investigate and to date incredibly difficult target for therapeutic use[271].

4.4 Materials and methods

4.4.1 Materials

Chemicals

Acetic anhydride was obtained from Merck and Amicon filters and Pyridine from Sigma Aldrich. Potassium cyanate was obtained from Alfa Aesar. CHAPS (Catalogue number: SC-29088) was obtained from SantaCruz. DTT was obtained from Biochemica Applichem and MES from Acros Organics. Cy5-alkyne and TAMRA-azide fluorophores, TTMA and THPTA ligands and Coomassie brilliant blue solution were synthesized in-house.

Antibodies

The antibodies used for western blotting: polyclonal rabbit anti His IgG antibody, Dako, P0448 and the secondary antibody was Goat anti-rabbit IgG-HRP antibody, BioRad Laboratories Ltd.,170-6515.

Proteins

The proteases supplied by R & D were provided with detailed instructions, which were followed. The final concentration of protease was 4-fold higher than recommended in order to provide workable conditions for the kinetic measurements. Cathepsin B (Catalogue number: 965-CY), cathepsin D (Catalogue number: 1029-AS), cathepsin L (Catalogue number: 1515-CY), cathepsin S (Catalogue number: 1183-CY), rhAEP

(Catalogue number: 2199-CY) and rmAEP (Catalogue number: 2058-CY) were obtained from R & D systems. Cathepsin K (Catalogue number: LS-G11893) was obtained from LifeSpan BioSciences. Bacterial Vin and its modified versions were produced and purified in-house. wt-Ova protein was obtained from Worthington (Catalogue number: LS-003054). Recombinant PAD4 was purchased from Sigma Aldrich).

Other

The silver staining kit was obtained from SilverQuest (Catalogue number; LC6070). Buffers such as 1 M Tris base, PBS, 5 M NaCl, 5 M HCl, 5 M NaOH, 87 % glycerol, sodium acetate, 1 M Hepes and 4x concentrated Lämmli buffer as sample buffer were prepared by hand in-house.

4.4.2   Methods

Protein production of vinculin

The plasmid (pET3d, Amp^R, Novagen) for the gene expression of wildtype Vinculin$_{435-743}$ (Met-Vin) was provided by Prof. Dr. Rene E. M. Toes (Department of Rheumatology, LUMC, Leiden, the Netherlands). The construct contained an N-terminal purification-tag (HPHHHHHHHH) for Ni-NTA purification and an enterokinase cleavage site (DDDDKH) for removal of the purification tag. The plasmid was transformed into a methionine auxotroph expression strain, namely *E. coli* B834(DE3) (met-aux, Genotype: F- ompT hsdSB (rB- mB-) gal dcm met(DE3), Novagen, cat 69041). For the expression of the Met-Vin, a single colony was picked. An expression on small scale (10-100 mL LB-Medium) was performed for each variant before up scaling (2-4 L of LB-Medium). 100 mL over night culture (O/N, ampicillin 50 μg/mL, 18 h, 37 ˚C, and 150 rpm) was used for the inoculation of 1 L LB medium (ampicillin 50 μg/mL, 37 ˚C, 150 rpm). The cells were grown until OD$_{600}$ nm 0.6-1.0 and induced with 1 mM isopropyl-β-D-1-thiogalactopyranoside (IPTG) for 18 h (30 ˚C, 150 rpm). Subsequently, cells were harvested by centrifugation (4000 g, 20 min, 4 ˚C), washed once with Tris-buffered saline (TBS); 50 mM Tris-HCl, 300 mM NaCl, pH 8.0) and stored at -80 ˚C for further use.

Protein purification of vinculin

Cell pellets were weighed, resuspended in TBS to 1-4 g/mL, prior to lysis by French Press (1.8-1.9 kbar, Stansted, Pressure Cell Homogeniser). Lysed cells were centrifuged (15,000 g, 1 h, 4 ˚C). The soluble fraction was then loaded onto a Ni-NTA affinity resin (Thermo Fisher Scientific, catalogue no. 88221) pre-equilibrated with TBS. After incubation for 1 h under gentle rotation, the beads were first washed with 2 CV of washing buffer 1 (TBS, 10 mM imidazole, pH 8.0) and subsequently with 3 CV washing buffer 2 (TBS with 50 mM imidazole). The resin was then treated with elution buffer (TBS, 250 mM imidazole, pH 8.0, 2 mL) to obtain the protein of interest (POI) in   10 mg/mL, which was then exchanged into protein buffer using a Sephadex G25 resin (PD-10 column; GE Healthcare). Purity of the POI was then determined using SDS-PAGE.

Carbamylation of proteins

Protein was carbamylated using a protocol adapted from Fando et al.[272]. Briefly, protein was reacted with 0.2M potassium cyanate (KOCN) in H_2O in a 1:1 v/v ratio for 24 h at 37 ˚C over night. The reaction progress was analyzed by LC-MS (Waters UPLC). Upon completion of the reaction, carbamylated proteins were purified by gel filtration over Sephadex G-25 (PD-10 pre-packed column, GE Healthcare). Purified proteins were stored at - 80 ˚C until further use.

Citrullination of proteins

Protein was citrullinated as follows; 1 mg/mL of protein was dissolved in Tris-HCl buffer (100 mM, pH 7.6) containing $CaCl_2$ in ddH_2O (10 mM) and DTT in DMSO (5 mM). Recombinant PAD4 was added to the reaction mixture at a concentration of 1 U. Samples were incubated at 37 ˚C for 5 h - over night under constant shaking (400 rpm). Upon completion of the reaction, citrullinated protein samples were purified via gel filtration and stored at -80 ˚C for further use.

Protein samples

Proteins were generally buffer exchanged into respective assay buffer after purification. The volume used for the samples contained 5 μg total. To get a more basic pH 1 M NaOH was added to the samples.

Activation of the proteases

The proteases obtained from R & D were activated according to the description of the manufacturer. Table 4.1 shows the general information, the used buffers and the final concentrations of activated proteases in solution used for the experiments. In general, the used protease concentration is 4x higher than what the manufacturer suggested.

Protease assay

The respective proteins were diluted further to a 20 μM concentration in the matching assay buffer described under cathepsin activation. In a 1:1 (v/v) ratio the activated cathepsin was added to the diluted protein, mixed and incubated at 37 ˚C in a thermo shaker at 300 rpm. The samples (15 μg) were taken at set time points after a short spin down to remove condensed fluids from the cap. The samples were incubated for 15 min at 90 ˚C in a thermo shaker with a heating cap to inactivate the endo-lysosomal proteases, frozen with liquid nitrogen and stored at -80 ˚C.

Sodium dodecyl sulphate-polyacrylamide gel electrophoresis

For SDS-PAGE analysis all samples were heated for 5 min at 95 ˚C. Heating the samples was omitted when bioorthogonal labelling mixture was added to avoid unspecific labelling. After a quick spin and manual resuspension 20 μl of each sample was loaded onto 1.5 mm, 15 % SDS-PAGE gel and run for 50 min at constant 250 V in the dark, if necessary. Subsequently, fluorescence densitometry was done at the appropriate wavelengths after which a Coomassie staining or silver staining was performed. Unless mentioned otherwise, the sample buffer used to load the samples on gels did not

Table 4.4: General information about the used buffers, specific activity and final concentration of the activated proteases.

	rm Cathepsin D	rm Cathepsin L	rh Cathepsin S	rh AEP
Specific activity [pmol/min/μg]	>600	>5,000	>300	>250
Activation buffer [mM/pH]	0.1M NaOAc, 0.2M NaCl, pH 3.5	50mM Nacitrate, 150mM NaCl, 1mM EDTA, 0.615% CHAPS, pH 3.0	50mM NaOAc, 5mM DTT, 250mM NaCl, pH 4.5	50mM NaOAc, 100mM NaCl, pH 4.0
Activation time [min]	10	60	120	120
Temperature [°C]	22	22	22	37
Assay buffer [mM, pH]	0.1M NaOAc, 0.2M NaCl, pH 3.5	25mM MES, 5mM DTT, pH 6.0	50mM NaOAc, 5mM DTT, 250mM NaCl, pH 4.5	50mM MES, 250mM NaCl, pH 5.0
c_{final} activated protease ‡ [ng/μL]	1.6	0.20	2.0	4.0

rh = recombinant human, c = concentration

‡ the final concentration of protease is diluted 1:1 (v/v) with protein solution to start the reaction.

contain DTT or β-mercaptoethanol in the experiments, which means that dimers and aggregates are visible on gel and in each lane 5 μg protein is loaded. In all experiments a negative control (-) was taken along, which represents protein incubated without the recombinant proteases, the respective volume was replaced by the respective assay buffer instead to keep the pH constant, but otherwise samples were treated exactly the same and heated along with the other samples over night. The gels were stained with a silver staining kit or with Coomassie brilliant blue. Protein samples containing UAAs, Aha or Hpg, respective fluorophores were ligated using CuAAC for fluorescence readouts.

Click-chemistry

30 μl of 1 M ascorbate was added to 51.2 μl of 0.1 M CuSO$_4$, both diluted in water. Followed by the addition of 10 μl 0.1 M TTMA[235] in DMSO, 706.5 μl of 0.1 M Hepes, pH 8.0 and 0.5 μl of a 2 mM solution of the respective alkyne-Cy5 or azide-TAMRA fluorophore in DMSO to the cocktail. The bioorthogonal labelling mixture was added in a 1:1 (v/v) ratio to the samples and was incubated for 30 min in the dark at rt. To stop the reaction, sample buffer was added and the samples were loaded on SDS-PAGE gels which were subsequently treated as stated above.

Circular dichroism

CD was performed as earlier described in Chapter 3.4.2.